

# THE KINETICS OF NON-ISOTHERMAL DECOMPOSITION OF PERIWINKLE SHELL

Akande, H. F.\*\*, Oyawoye, M.R.\* , Ibrahim, A.A.\*\* and Nwafulugo, F. U.\*

\*Department of Chemical Engineering, Kaduna Polytechnic, Kaduna, Nigeria

\*\*Department of Mechanical Engineering, Kaduna Polytechnic, Kaduna, Nigeria

+ Corresponding author: [hassan.akande@kadunapolytechnic.edu.ng](mailto:hassan.akande@kadunapolytechnic.edu.ng)

**Abstract**—The paper presents the kinetic studies of periwinkle shell thermal decomposition. Non-isothermal thermogravimetric experiments were carried out at heating rates of 10, 20 and 30 °C/min. For the estimation of activation energy ( $E$ ), Kissinger-Akahira-Sinose (KAS), Ozawa-Flynn-Wall (OFW) and Coats-Redfern methods were used. The results showed that while KAS and OFW methods produced  $E$  values of 1349.97 and -1267.08 kJ/mol respectively with a corresponding correlation coefficient ( $R^2$ ) values of 0.9919 and 0.9917, Coats-Redfern method produced better  $R^2$  value with  $E$  value ranges between 146.43 and 156.20 kJ/mol. Using the Coats-Redfern method, contracting area ( $R2$ ) model produced the most suitable model to represent the reaction's mechanism. The values of activation energy decrease with increasing heating rate.

**Index Terms**—Calcium carbonate, Kinetic parameters, Non-isothermal thermogravimetry, Periwinkle shell, Quicklime, Recycling, Thermal decomposition

## 1 INTRODUCTION

RECYCLING is one of the environmental waste management schemes that is considered adequate for attaining a sustainable development; it produces new and useful commodities from wastes thereby reducing the exploitation of raw materials. One of such wastes is the shell of molluscs such as cockle, oyster, mussel, snail and periwinkle. According to Wanninger and Wollesen (2018), molluscs have inhabited almost all the terrestrial and aquatic parts of the world; this suggests their population which has a direct effect on the shell (waste) generated to the environment. Many works (Chilakala *et al.*, 2019; Filhoa *et al.*, 2014; Nagasawa, 2013; Marin *et al.*, 2012) have established that these shells are rich in calcium carbonate ( $\text{CaCO}_3$ ) mineral in a proportion comparable to that of limestone. Periwinkle is abundantly found in the delta region of Nigeria (Niger Delta) (Ogunola *et al.*, 2017); *Tympanotonus fuscatus* and *Pachymelania aurita* are the main species inhabiting the littoral region (Bob-Manuel, 2012). Usually, humans throw the periwinkle shell into the environment after consuming their meat (Malu and Basse, 2004). An essential way of carrying out recycling of mollusc shells is through thermal decomposition: the shell is heated to a certain temperature whereby its  $\text{CaCO}_3$  component decomposes to  $\text{CaO}$  and letting-off carbon (IV) oxide ( $\text{CO}_2$ ) gas (Mohamed *et al.*, 2012). Thermal decomposition of  $\text{CaCO}_3$  resources is also referred to as calcination (Mohamed *et al.*, 2012).

Calcination of  $\text{CaCO}_3$  resources such as limestone (Ar and Dogu, 2001) and mollusc shells have been widely investigated due to its importance to industrial processes like cement production and quicklime ( $\text{CaO}$ ) production; especially, kinetic analysis of the reaction has received much attention. The kinetic analysis is generally based on the experimental methods as well as the computational methods (Tian *et al.*, 2017). The experimental method of studying calcination is mainly isothermal or non-isothermal thermogravimetric analysis. These experimental methods have been well reported in the literature, and various computational methods have been used for evaluating the kinetic parameters (Brown *et al.*, 2000; Vyazovkin *et al.*, 2011); all these works aim at attaining the most probable representation of the process. The commonly investigated types of the mollusc are cockle (Mohamad *et al.*, 2016), oyster (Soisuwan *et al.*, 2014) and mussel (Zhang *et al.*, 2013) while periwinkle shell has received scanty attention.

Kinetic analysis of thermal decomposition of the periwinkle shell determines the reaction's kinetic parameters. They are the activation energy ( $E$ ), Arrhenius constant ( $A$ ) and the reaction model ( $f(a)$ ). These parameters are known as the kinetic triplet (Kok, 2015). Many related works found in the literature simply focused on the potential use of the periwinkle shell in the construction industry and some other necessary uses (Ohimain *et al.*, 2009; Olusola and Umoh, 2012; Otunyo *et al.*, 2013; Oyedepo and Olukanni, 2015 and Soneye *et al.*, 2016). Studies on the kinetics of periwinkle shell calcination have not received much attention; therefore, the aim of this work was to further the current knowledge in this area.

- Dr. Hassan F. Akande has PhD. in Chemical Engineering from Federal University of Technology, Minna, Nigeria, +234 8033686645. E-mail: [hassan.akande@kadunapolytechnic.edu.ng](mailto:hassan.akande@kadunapolytechnic.edu.ng)
- Dr. Francisca Nwafulugo has PhD. in Chemical Engineering from Ahmadu Bello University, Zaria, Nigeria, +234 8033686645. E-mail: [hassan.akande@kadunapolytechnic.edu.ng](mailto:hassan.akande@kadunapolytechnic.edu.ng)

## 2 MATERIAL AND METHODS

### 2.1 Material

The periwinkle shell was crushed using a crusher and then washed with tap water. The sample was dried to constant mass (in the sun) for six days. After that, the sample was ground and sieved to a particle size of 0.1 mm.

### 2.2 Calcination Method

The calcination characteristic of the sample was obtained through the thermogravimetric analysis (TGA). A mass of 10 mg of the sample was placed on the sample holder of the Thermogravimetric (TG) machine (LINSEIS L7Q2171STGA). Calcination of the sample was done in an atmosphere of 20 ml N<sub>2</sub>/min. The heating rate for the calcination process was at 10, 20 and 30 K/min, respectively.

### 2.3 Kinetic Method

The general rate equation of solid-state reaction kinetics is expressed in Equation (1)

The general rate equation of solid-state reaction kinetics is expressed in Equation (1)

$$\frac{d\alpha}{dt} = k(T)f(\alpha) \quad (1)$$

where  $d\alpha/dt$  is the rate of the decomposition reaction,  $f(\alpha)$  is a function of conversion of the sample (a symbol for the reaction mechanism).

Arrhenius constant in Equation (1) is expressed as

$$k(T) = Ae^{-\frac{E}{RT}} \quad (2)$$

where E is the activation energy (kJ/mol), A is the frequency factor (min<sup>-1</sup>) and R is the universal gas constant (8.314 kJ/mol K). This re-expresses Equation (1) as

$$\frac{d\alpha}{dt} = Ae^{-\frac{E}{RT}}f(\alpha) \quad (3)$$

The relationship of time and temperature with regards to isothermal and non-isothermal measurements can be expressed as

$$\beta = \frac{dT}{dt} \quad (4)$$

where  $\beta$  is the heating rate (°C/min) of sample imposed by the equipment,  $\frac{dT}{dt}$  rate of change of temperature. The combination of Equations (3) and (4) produces the constant heating rate, non-isothermal differential equation

$$\frac{d\alpha}{dT} = \frac{A}{\beta} e^{-\frac{E}{RT}}f(\alpha) \quad (5)$$

The data from non-isothermal TGA is converted to fractional decomposition ( $\alpha$ ) expressed in Equation (6)

$$\alpha = \frac{M_i - M_T}{M_i - M_f} \quad (6)$$

where  $M_i$  - the initial mass of the sample;  $M_T$  - the mass of the sample at any temperature T and  $M_f$  - final mass at the end of the reaction.

### 2.4 NON-ISOTHERMAL COMPUTATION METHODS

The computation methods that are suitable for evaluating the kinetic parameters from non-isothermal data were used; Coats-Redfern, Kissinger-Akahira-Sinose (KAS) and Ozawa-Flynn-Wall (OFW) are prominent examples (Lei *et al.*, 2019; Khawam, 2007). The appropriateness of each of these models to the calcination data of the sample was examined.

The Coats-Redfern method involves fitting of various reaction

models to the calcination data—a method called model-fitting. Coats-Redfern is obtained from the integral of Equation (5) as

$$\ln \left[ \frac{g(\alpha)}{T^2} \right] = \ln \left[ \frac{AR}{\beta T} \left( 1 - \frac{2RT}{E} \right) \right] - \frac{E}{RT} \quad (6)$$

Thus, E was evaluated from the slope while A can be evaluated from the intercept from the plot of  $\ln \left[ \frac{g(\alpha)}{T^2} \right]$  against  $\frac{E}{RT}$  of Equation (6) (Ashraf *et al.*, 2019). Some solid-state reaction models in both differential ( $f(\alpha)$ ) and ( $g(\alpha)$ ) forms are presented in Table 1.

Kissinger-Akahira-Sinose (KAS) and Ozawa-Flynn-Wall (OFW) methods do not rely on the prior knowledge of the reaction model in order to estimate the kinetic parameters; these are called model-free methods. Equations (6 and 7) express KAS and OFW respectively (Lei *et al.*, 2019).

$$\ln \left[ \frac{\beta}{T^2} \right] = \ln \left[ \frac{RA}{Eg(\alpha)\beta} \right] - \frac{E}{RT} \quad (6)$$

$$\ln(\beta) = -1.052 \frac{E}{RT} + \ln \left[ \frac{AE}{Rg(\alpha)} \right] \quad (7)$$

Table 1: Some solid-state reaction models

Model/ Mechanism	Differential form $f(\alpha) = 1/(k d\alpha/dt)$	Integral form $g(\alpha) = kt$
<b>Reaction order models</b>		
Zero-order (F0/R1)	$(1 - \alpha)^0$	$\alpha$
First-order (F1)	$1 - \alpha$	$-\ln(1 - \alpha)$
Second-order (F2)	$(1 - \alpha)^2$	$[1/(1 - \alpha)] - 1$
Third-order (F3)	$(1 - \alpha)^3$	$(1/2)[(1 - \alpha)^{-2} - 1]$
<b>Geometrical contraction models</b>		
Contracting area (R2)	$2(1 - \alpha)^{1/2}$	$1 - (1 - \alpha)^{1/2}$
Contracting volume (R3)	$3(1 - \alpha)^{2/3}$	$1 - (1 - \alpha)^{1/3}$
<b>Diffusion models</b>		
1-D diffusion (D1)	$1/(2\alpha)$	$\alpha^2$
2-D diffusion (D2)	$-[1/\ln(1 - \alpha)]$	$[(1 - \alpha)\ln(1 - \alpha)] + \alpha$
3-D diffusion - Jander (D3)	$[3(1 - \alpha)^{2/3}]/[2(1 - (1 - \alpha)^{1/3})]$	$(1 - (1 - \alpha)^{1/3})^2$
Ginstlin g-Brounshstein (D4)	$3/[2((1 - \alpha)^{-1/3} - 1)]$	$1 - (2/3)\alpha - (1 - \alpha)^{2/3}$
<b>Nucleation models</b>		
Mampel power law (P2)	$2\alpha^{1/2}$	$\alpha^{1/2}$
Mampel power law (P3)	$3\alpha^{2/3}$	$\alpha^{1/3}$
Mampel power law (P4)	$4\alpha^{3/4}$	$\alpha^{1/4}$
Exponential law Avrami-Erofeyev (A2)	$\alpha$	$\ln \alpha$
Avrami-Erofeyev (A2)	$2(1 - \alpha)[- \ln(1 - \alpha)]^{1/2}$	$[- \ln(1 - \alpha)]^{1/2}$
Avrami-Erofeyev (A3)	$3(1 - \alpha)[- \ln(1 - \alpha)]^{2/3}$	$[- \ln(1 - \alpha)]^{2/3}$

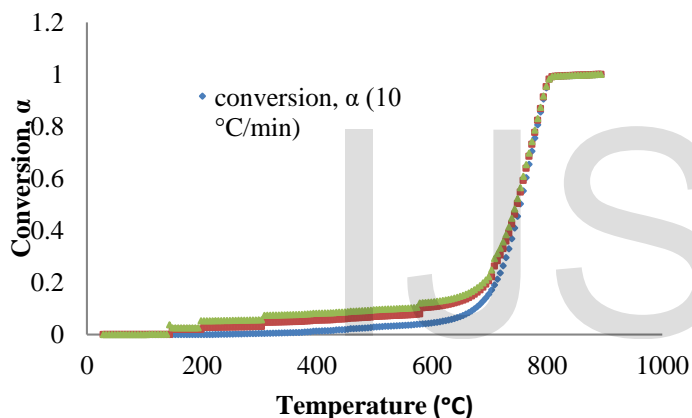
Avrami-Erofeev (A4)	$4(1 - \alpha)[-ln(1 - \alpha)]^{3/4}$	$[-ln(1 - \alpha)]^{3/4}$
Prout-Tompkins (B1)	$\alpha(1 - \alpha)$	$ln[\alpha/(1 - \alpha)] + c^a$

(Khawam and Flanagan, 2006; Rejitha, 2010)

### 3 RESULTS AND DISCUSSION

#### 3.1 THERMAL DECOMPOSITION (CALCINATION) OF PERIWINKLE SHELL

The thermal decomposition process of the periwinkle shell sample is presented in Figure 1. It is seen that the initial stage of mass-loss occurred in the range of 200 - 650 °C. This could be due to the vapourisation of moisture from the periwinkle shell sample. Also, it is seen that the heating rates of 10, 20 and 30 °C/min resulted in increased conversion in the same order. Another stage of rapid mass-loss occurred in the range of 670 - 790 °C, substantially due to thermal decomposition of the sample. These observations are similar to the reports of Pliya and Cree (2015) and Mohamad *et al.* (2016).



This could be due to the vapourisation of moisture from the periwinkle shell sample. Also, it is seen that the heating rates of 10, 20 and 30 °C/min resulted in increased conversion in the same order. Another stage of rapid mass-loss occurred in the range of 670 - 790 °C, substantially due to thermal decomposition of the sample. These observations are similar to the reports of Pliya and Cree (2015) and Mohamad *et al.* (2016).

#### 3.2 KINETIC ANALYSIS OF THE CALCINATION

The results of the activation energy (E) obtained through the use of Ozawa-Flynn-Wall (OFW) and Kissinger-Akahira-Sunose (KAS) models are presented in Table 2. Using these models, E was estimated at a fractional conversion value of 0.5. OFW model produced a curve with a poorer fit than that of KAS; the Equation of its curve does not obey the OFW model (Equation (7)).

Table 2: Ozawa-Flynn-Wall (OFW) and Kissinger-Akahira-Sunose (KAS) models

Model	E (kJ/ mol K)	Equation of the curve	R <sup>2</sup>
OFW	-1267.08	y = 160328x - 154.06	0.9917
KAS	1349.97	y = -162373x + 169.91	0.9919

The results obtained through the Coats-Redfern model are presented in Tables 3 through 6 (for the heating rates of 10, 20 and 30 °C/min respectively). As seen in Tables 4 and 5, contracting area (R2) and 3-D diffusion -Jander (D3) respectively have the highest correlation coefficients (R<sup>2</sup>) of 0.9999: this R<sup>2</sup> value occurs at the heating rate values of 20 and 30 °C/min for the R2 model while it occurs only at 10 °C/min for the D3 model. R2 model also shows good fitting at 10 °C/min with R<sup>2</sup> value of 0.9993. Thus, it is chosen as the most probable model for describing the calcination of periwinkle shell in this study. This result is similar to the findings of Lei *et al.* (2019). The values of activation energy is also seen to decrease with increasing heating rate which means that at higher heating rates, periwinkle shell calcination is favoured.

Table 3: Reaction order

Model	β(°C/min)	E(kJ/mol K)	A	Equation of the curve	R <sup>2</sup>
F0/R1	10	146.1	12.703793	Y = -17573x + 2.5419	0.995
				Y = -14336x - 0.5184	0.997
				Y = -13214x - 1.5771	0.997
	20	119.1	0.595473	Y = -27544x + 12.606	0.999
				Y = -24132x + 9.4165	0.998
				Y = -22938x + 8.3039	0.998
	30	109.8	0.2065733	Y = -40788x + 25.913	0.994
				Y = -37551x + 22.947	0.990
				Y = -36429x + 21.928	0.989
F1	10	229.0	298343.3	Y = -57035x + 42.198	0.985
				Y = -54241x + 39.729	0.981
				Y = -53301x + 38.914	0.979
	20	200.6	12289.495	Y = -40788x + 25.913	0.994
				Y = -37551x + 22.947	0.990
				Y = -36429x + 21.928	0.989
	30	190.7	4039.5966	Y = -57035x + 42.198	0.985
				Y = -54241x + 39.729	0.981
				Y = -53301x + 38.914	0.979
F2	10	339.1	1.79421E+11	Y = -40788x + 25.913	0.994
				Y = -37551x + 22.947	0.990
				Y = -36429x + 21.928	0.989
	20	312.2	924177748	Y = -57035x + 42.198	0.985
				Y = -54241x + 39.729	0.981
				Y = -53301x + 38.914	0.979
	30	302.8	333587233	Y = -40788x + 25.913	0.994
				Y = -37551x + 22.947	0.990
				Y = -36429x + 21.928	0.989
F3	10	474.1	2.12011E+18	Y = -57035x + 42.198	0.985
				Y = -54241x + 39.729	0.981
				Y = -53301x + 38.914	0.979
	20	450.9	1.79509E+17	Y = -40788x + 25.913	0.994
				Y = -37551x + 22.947	0.990
				Y = -36429x + 21.928	0.989
	30	443.1	7.94576E+16	Y = -57035x + 42.198	0.985
				Y = -54241x + 39.729	0.981
				Y = -53301x + 38.914	0.979

Table 4: Geometrical contraction

Model	$\beta(^{\circ}\text{C}/\text{min})$	E (kJ/mol K)	A	Equation of the curve	$R^2$
R2	10	184.19	651.7757	$y = -22154x + 6.4797$	0.9993
	20	156.20	27.45094	$y = -18788x + 3.3124$	0.9999
	30	146.43	9.107518	$y = -17612x + 2.2091$	0.9999
R3	10	198.36	2426.974	$y = -23859x + 7.7944$	0.9998
	20	170.17	100.4742	$y = -20468x + 4.6099$	0.9998
	30	160.31	33.09229	$y = -19282x + 3.4993$	0.9996

				$x + 25.968$	
	20	300.5	241.2901325	$y = -36149x + 19.662$	0.999
		4			5
	30	281.1	38570568.1	$y = -33817x + 17.468$	0.999
		5			7
D3	10	413.8	4.60616E+1	$y = -49776x + 31.461$	0.999
		4	3		9
	20	357.4	7902262617	$y = -42993x + 25.093$	0.999
		4	5		8
	30	337.7	8565428885	$y = -40622x + 22.871$	0.999
		3			6
D4	10	380.0	7.50496E+1	$y = -45710x + 27.344$	0.999
		3	1		4
	20	319.3	758611290	$y = -38407x + 20.447$	0.999
		2			8
	30	299.8	83553696.3	$y = -36060x + 18.241$	0.999
		1			9

Table 5: Diffusion

Mode l	$\beta(^{\circ}\text{C}/\text{min})$	E (kJ/mol K)	A	Equation of the curve	$R^2$
D1	10	309.3	1262046124	$y = -37204x + 20.956$	0.995
		1			7
	20	255.4	2774552.717	$y = -30730x + 14.836$	0.997
		9			7
	30	236.8	334034.675	$y = -28486x + 12.719$	0.998
		3			2
D2	10	356.1	1.89565E+1	$y = -42839x + 12.719$	0.998
		6	1		4

Table 6: Nucleation

Mode l	$\beta(^{\circ}\text{C}/\text{min})$	E (kJ/mol K)	A	Equation of the curve	$R^2$
P2	10	146.1	6.35156136	$y = -17573x + 1.8487$	0.995
		0	3		1
	20	119.1	0.29775046	$y = -14336x - 1.2115$	0.997
		9	8		3
	30	109.8	0.103292	$y = -13214x - 1.2115$	0.997
		6			9

P3	10	37.30	5.92059E-05	2.2702 y = - 0.991 4485.9 3 x - 9.7345
	20	28.32	2.13386E-05	y = - 3406.8 0.994 x - 4 10.755
	30	25.22	1.5007E-05	y = - 0.995 3032.9 3 x - 11.107
P4	10	23.69	1.27628E-05	y = - 0.987 2850x - 7 11.269
	20	16.97	5.93897E-06	y = - 0.991 2040.6 x - 12.034
	30	14.63	4.5564E-06	y = - 0.991 1760.2 9 x - 12.299
A2	10	105.9	0.19522574	y = - 0.999 12743x 8 -
	20	91.76	0.039633	1.6336 y = - 0.998 11037x 5 -
	30	86.80	0.02272250	3.2281 y = - 0.997 10440x 7 -
A3	10	146.9	22.48393	3.7844 y = - 0.999 17677x 8 +
	20	128.0	241.290218	3.1128 y = - 0.998 15402x 6 +
	30	121.4	1.27774949	0.9868 y = - 0.997 14606x 9 +
A4	10	167.4	241.2902	0.2451 y = - 0.999 20144x 8 + 5.486

20	146.2	22.06958	y = - 0.998 17585x 6 +
30	138.7	22.4839168	3.0942 y = - 0.997 16689x 9 +
			2.2598

#### 4. Conclusion

The Coats-Redfern method provides better fitting to the non-isothermal TGA data of periwinkle shell than KAS and OFW models. Using the Coats-Redfern method, contracting area (R2) model is the most suitable model to represent the reaction's mechanism. The activation energy values range between 146.43 and 156.20 kJ/mol. The values of activation energy decrease with increasing heating rate.

#### 5. ACKNOWLEDGMENT

The authors are grateful to the Tertiary Education Trust Fund (TETFUND), Abuja, Nigeria for providing the Institutional Based Research (IBR) grant for this work.

#### REFERENCES

- [1] J.S. Bridle, "Probabilistic Interpretation of Feedforward Classification Network Outputs, with Relationships to Statistical Pattern Recognition," *Neurocomputing - Algorithms, Architectures and Applications*, F. Fogelman-Soulie and J. Herault, eds., NATO ASI Series F68, Berlin: Springer-Verlag, pp. 227-236, 1989. (Book style with paper title and editor)
- [2] W.-K. Chen, *Linear Networks and Systems*. Belmont, Calif.: Wadsworth, pp. 123-135, 1993. (Book style)
- [3] H. Poor, "A Hypertext History of Multiuser Dimensions," *MUD History*, <http://www.ccs.neu.edu/home/pb/mud-history.html>. 1986. (URL link \*include year)
- [4] K. Elissa, "An Overview of Decision Theory," unpublished. (Unpublished manuscript)
- [5] R. Nicole, "The Last Word on Decision Theory," *J. Computer Vision*, submitted for publication. (Pending publication)
- [6] C. J. Kaufman, Rocky Mountain Research Laboratories, Boulder, Colo., personal communication, 1992. (Personal communication)
- [7] D.S. Coming and O.G. Staadt, "Velocity-Aligned Discrete Oriented Polytopes for Dynamic Collision Detection," *IEEE Trans. Visualization and Computer Graphics*, vol. 14, no. 1, pp. 1-12, Jan/Feb 2008, doi:10.1109/TVCG.2007.70405. (IEEE Transactions)
- [8] S.P. Bingulac, "On the Compatibility of Adaptive Controllers," *Proc. Fourth Ann. Allerton Conf. Circuits and Systems Theory*, pp. 8-16, 1994. (Conference proceedings)
- [9] H. Goto, Y. Hasegawa, and M. Tanaka, "Efficient Scheduling Focusing on the Duality of MPL Representation," *Proc. IEEE Symp. Computational Intelligence in Scheduling (SCIS '07)*, pp. 57-64, Apr. 2007, doi:10.1109/SCIS.2007.367670. (Conference proceedings)
- [10] J. Williams, "Narrow-Band Analyzer," PhD dissertation, Dept. of Elec-

- trical Eng., Harvard Univ., Cambridge, Mass., 1993. (Thesis or dissertation)
- [11] E.E. Reber, R.L. Michell, and C.J. Carter, "Oxygen Absorption in the Earth's Atmosphere," Technical Report TR-0200 (420-46)-3, Aerospace Corp., Los Angeles, Calif., Nov. 1988. (Technical report with report number)
- [12] L. Hubert and P. Arabie, "Comparing Partitions," *J. Classification*, vol. 2, no. 4, pp. 193-218, Apr. 1985. (Journal or magazine citation)
- [13] R.J. Vidmar, "On the Use of Atmospheric Plasmas as Electromagnetic Reflectors," *IEEE Trans. Plasma Science*, vol. 21, no. 3, pp. 876-880, available at <http://www.halcyon.com/pub/journals/21ps03-vidmar>, Aug. 1992. (URL for Transaction, journal, or magazine)
- [14] J.M.P. Martinez, R.B. Llavori, M.J.A. Cabo, and T.B. Pedersen, "Integrating Data Warehouses with Web Data: A Survey," *IEEE Trans. Knowledge and Data Eng.*, preprint, 21 Dec. 2007, doi:10.1109/TKDE.2007.190746.(PrePrint)

IJSER